Automatically Deploy Deep Learning Models on FPGA

ABSTRACT

Deep learning has demonstrated great success in numerous applications such as image classification, speech recognition, video analysis, etc. However, deep learning models are much more computation-intensive and memory-intensive than previous shallow models, which makes their serving in large-scale data centers and real-time embedded systems big challenges. Considering performance, flexibility and energy-efficiency, FPGA-based accelerator for deep learning models is a promising solution. Unfortunately, conventional accelerator design flows make it hard for FPGA developers to keep up with the fast pace of innovations in deep learning.

In this paper, we propose an end-to-end framework that takes symbolic descriptions (TensorFlow in this work) of deep learning models as input, and automatically generates the hardware implementations on FPGA boards. We take an OpenCL HLS-based approach, and perform deep learning model inference with general-purpose computing kernels like GEMM, GEMV, etc. The framework automatically estimates the performance and resource utilization with the help of our proposed models, then chooses the optimal hardware configuration. Besides, we carefully design the processing units and data layout strategies for further optimizations. To show the great effectiveness and state-of-the-art performance provided by our proposed framework, we implement ANNs, CNNs and RNNs as our case studies.

Keywords

FPGA, TensorFlow, Compiler, Accelerator

1. INTRODUCTION

Deep learning models have raised a new storm of artificial intelligence, and achieved great improvements in several domains such as computer version[cite], speech recognition[cite], natural language processing[cite], etc. Inspired by the impressive breakthroughs achieved by deep learning models, many researchers in both academic and industry are studying in or integrating their work with powerful deep learning models. With their model accuracy closer to or even better than human, deep learning models are more and more deployed at scale in data centers by leading companies [Google translate APIs, Microsoft Cognitive Services], as well as in embedded systems like mobile phones and robots.

Deep learning models are well-known to be computation-intensive and memory-intensive because of their deep topological structures, complicated neural connections and massive data to process. These characteristics indicate that deploying pre-trained deep learning models with high performance and good energy efficiency becomes a big challenge. To solve this problem, many heterogeneous accelerators for deep learning model inference have been investigated recently. They are mainly based on GPU[cite], ASIC[cite] and FPGA [cite]. Among these designs, FPGA-based accelerators received great popularity with their strong flexibility and good energy efficiency.

Unfortunately, hand-coded FPGA-based accelerator faces both productivity and programmability challenges for deploying deep learning models in real applications. On the one hand, the design and optimization work of FPGA-based accelerator is quite heavy, which will typically cost a single professional hardware developer several weeks to migrate a deep learning model onto FPGA, even with the help of high-level synthesis tools. For deep learning model designers, there is no programming interfaces or libraries (like cuBLAS[cite?] and cuDNN[cite?] in Nvidia GPUs) to easily and fast migrate their model to FPGAs. On the other hand, prior work on FPGA-based accelerator for deep learning models focus on accelerating certain type of layers[cite] or certain models[cite]. Since deep learning evolves rapidly, various model configurations and optimization techniques are emerging so fast that re-designing FPGA-based accelerator for every new model or technique is quite clumsy and inefficient.

According to the analysis above, there is a strong demand for an easy-to-use framework which can fast migrate deep learning models to FPGA implementations. In this paper, we propose a framework which takes symbolic descriptions (using TensorFlow) of deep learning models as input, and outputs implementations of the corresponding FPGA-based accelerators for model inference. The accelerators are implemented by OpenCL-based HLS, and we convert model inference into general-purpose computations like GEMM, GEMV, etc. Several performance and resource models are developed and invoked to ensure the functionality, performance and energy efficiency of the implemented accelerator. The whole compilation procedure is end-to-end and automated, which makes it possible for all deep learning researchers and users to use FPGA as a common device to perform model inference.

We make the following contributions in this paper:

- We offer a thorough analysis of factors affecting the performace on each function of DNN and propose the optimal solution on FPGA.

- We build a framework which compiles deep learning models described in TensorFlow to FPGA implementation for model inference, and we test it with ANNs, CNNs and RNNs. Compared with previous accelerating work, this automated framework can save XXx design time on average.

- We implement high-performance matrix multiplication kernels for model inference, and carefully design the data layout strategies for further optimization. Several estimation models for performance and resource utilization are proposed, and our framework takes advantage of these models to explore the whole design space, and choose the optimal configuration as the final implementation.

- We implement several deep learning models as case studies. The experimental results shows that our symbolic compiler offers great effectiveness, and the final FPGA-based accelerators show state-of-the-art performance and energy efficiency.

The rest of this paper is organized as follows: Section 2 introduces some basis of deep learning models, TensorFlow and OpenCL-based HLS. Section 3 describes detailed architecture of our proposed framework, then the hardware implementation and design space exploration are introduced in Section 4. In Section 5, we show the experimental setup and results of our case studies. At last, Section 6 concludes this paper and discusses about future work.

2. BACKGROUND

In this section, we first introduce the characteristics of deep learning model inference, and the corresponding difficulties in hardware implementation. Then we provide some basis for TensorFlow and OpenCl-based HLS architecture.

2.1 Deep Learning models

Deep learning has evolved into a big community, and many interesting and powerful models have been proposed. These models can be divided into several categories. By topological structure, we can divide these models into Feed-Forward Neural Networks (FFNNs), Convolutional Neural Networks (CNNs), Recurrent Neural Networks (RNNs), etc [Figure?]. All these models are comprised of several neural layers. By types of layers, we can have fully-connected layers, convolution layers, recurrent layers, pooling layers, activation layers, etc. A single deep learning model can choose any topological structure mentioned above, and it may includes several types of layers in its configuration. So this results in a huge design space of possible model configurations.

The great flexibility and diversity of deep learning model configuration is indeed good to inspire more powerful models and designs, while it is a nightmare for hardware developers who accelerating certain type of layers or models. For example, convolution layers are well-known to be computation-intensive, while fully-connected layers and recurrent layers

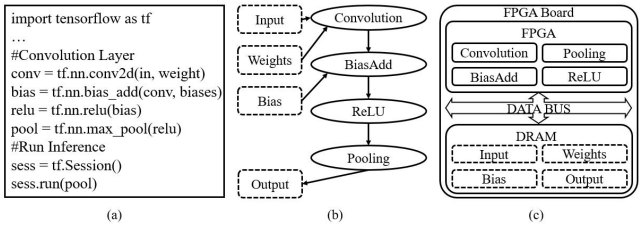

Figure 1: Comparison between TensorFlow and FPGA Implementation

are memory-intensive. Pooling layers and different activation layers needs additional operations and hardware modules. Besides, every time the model configuration changes, the hardware developers have to work hard to modify or even re-design their implementations.

2.2 Deep Learning Frameworks

Many open-source frameworks have been released for deep learning research, like TensorFlow [1], Caffe [8], Theano [2], etc. All these frameworks bring great convenience for deep learning model designing, training and deploying on CPUs and GPUs, while their migration to FPGAs remain a blank. Different from the other frameworks, TensorFlow runs in a symbolic style, and it performs computations in a hardware-similar way: All the computations described in TensorFlow can be transformed into a data flow graph, with each node in this graph representing a computation operation or a certain function. Data are viewed as tensors which stream across each node to get the final results of the whole computation. Besides, TensorFlow is a programming library , and can support much more types of deep learning models (ANN/CNN/RNN/...) as well as other scientific computation. Thus, we appreciate the concepts of tensor and data flow graph in TensorFlow, and we adopt similar strategies in our proposed framework.

2.3 OpenCL HLS

Numerous customized hardware accelerators for deep learning models have been proposed, but the implementation approach varies. Some of them are ASIC-based [3] [4] [15], and some of them are RTL-based FPGA accelerators [10]. However, the time and cost for ASIC design is usually not bearable for most developers, and it is well-known that using hardware description languages (e.g. Verilog, VHDL) to design FPGAs is quite hard and time-consuming. Besides, the learning curve for beginners in hardware development is very steep. These two reasons make hardware design a heavy work for researchers. Fortunately, high-level-synthesis (HLS) tools help us solve this difficult problem. These tools receive designs programmed in high-level programming languages (C, C++, OpenCL, etc.), then transform them into the corresponding HDL descriptions and get the final hardware configuration files. Thus, HLS-based FPGA accelerators wins great popularity for deep learning model inference [19] [17] [12]. Figure 2 shows a rough framework of the FPGA implementations designed by OpenCL-based HLS. Similar to other OpenCL-based frameworks, the whole system is comprised of two main parts: *Host* and *Device*. *Host* is a desktop computer or server, where a C/C++ program is compiled and executed to perform the controlling opera-

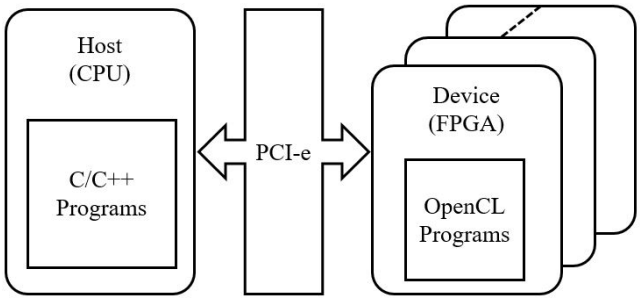

Figure 2: OpenCL-HLS Framework

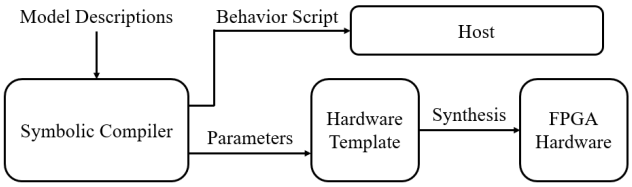

Figure 3: Overall Framework

tions. *Device* is an FPGA board, which is plugged into the motherboard of *Host* through a PCI-e slot. Data communication between *Host* and *Device* are accomplished through this PCI-e slot, and this slot is also used to power and program FPGA. Inside FPGA, hardware modules are compiled and invoked by *Host* to complete the main computation tasks.

3. FRAMEWORK

We introduce the architecture of our proposed framework in this section. We first give an overview, then discuss about the main parts of it separately.

3.1 Overview

An overview of our overall framework is shown in Figure 3.The whole framework is mainly comprised of three parts: *Symbolic Compiler*, *Host Dispatcher*, and *Hardware Generator*. *Symbolic Compiler* takes symbolic descriptions (similar to TensorFlow) of deep learning models as input. Through an analysing phase, *Symbolic Compiler* generates the behavior script for *Host Dispatcher* to execute, and decides certain implementation-related parameters for *Hardware Generator*. *Host Dispatcher* takes advantage of the behavior script to dispatch hardware kernels for model inference. *Hardware Generator* is composed of a set of elaborately designed OpenCL kernels to implement different deep learning functions. These kernels are designed model-agnostic and reconfigurable. With the parameters received from *Symbolic Compiler*, *Hardware Generator* instantiates hardware templates and generates corresponding OpenCL codes. The whole framework works in an "end-to-end" manner: from software-based model descriptions (TensorFlow codes) to FPGA-based model inference implementations (FPGA programming files), and this procedure is all done automatically without any human intervention.

3.2 Symbolic Compiler

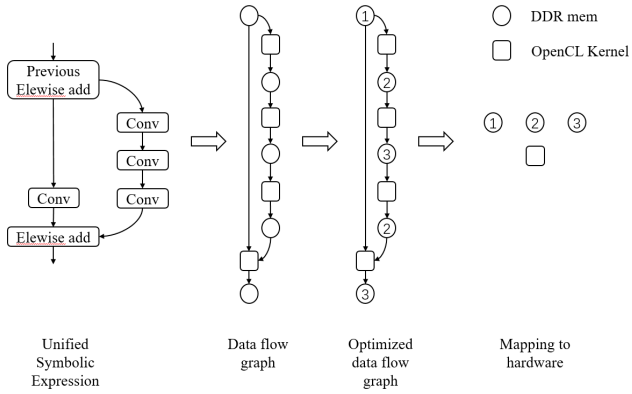

Figure 4: Compile Working Flow

Symbolic Compiler serves as the role to map arbitrary user-defined deep learning model into certain hardware implementations. We denote the way model described as Unified Symbolic Expression (USE for short). USE describes the topological structure and functionality of the models to be implemented on FPGA. Model descriptions in TensorFlow, Caffe and other deep learning frameworks can be easily converted into USE without much effort.

Figure **??** shows an example of the working flow of *Symbolic Compiler*. Figure **??** (a) shows the USE for a fraction of ResNet-152 [7]. *Symbolic Compiler* takes the USE and merges Element Wise Add layer with Convolution layer. It generates the data flow graph with computation nodes and data accessing nodes in Figure **??** (b). Due to the limitation on computation resource and DRAM storage, *Symbolic Compiler* must adopt resource reusing strategies. For computation resource reusing, *Symbolic Compiler* generates only one hardware instance for each type of computation node, and maps all computation nodes of the same type to their corresponding instances. For storage resource reusing, *Symbolic Compiler* divides DRAM into several data buffers, and reuses these buffers as long as no conflict occurs among these data accessing nodes.

This mapping problem in essence equals to the well-known register allocation problem in compiler theory: storage unit equals variables, and memory buer equals to register. [Cite] has proved this problem could be abstracted to a graph coloring problem. This graph coloring problem is NP hard and serveral heuristic algorithm has been proposed to optimize it. We choose DSATUR [Cite] algorithm as the solver for this problem.

4. HOST PROGRAM

Host program invokes OpenCL API.

5. HARDWARE TEMPLATE

The complex structure and the great variaty of deep learning models has bring big challege to generate optimal hardware for them individually. We address this challenge by the observation that deep learning models share similar structure on computation intensive layers, which can always be expressed as $M \times M$ or $M \times V$.

5.1 Hardware Generator

The great complexity and variability of deep learning model structures have brought big challenges to generating optimal hardware for them individually. We find that deep learning models are always constructed by stacked layers, and these layers share similar structure at computation part, which can always be expressed as or converted to matrix multiplication. As a result, we divide the operations inside each model layer into computation part and layer-specific part. For the computation part, we use a model-independent MM (Matrix Multiplication) kernel to perform the calculations. For layer-specific part, we implement data management kernel for each type of layer separately, which insures data are fed into MM kernel in a correct order. *Hardware Generator* stores the code templates for different types of layers, and instantiates templates for code generating with the optimized parameters received from *Symbolic Compiler*. We use a flexable General Purpose Matrix Multiplication (GEMM) engine to accerate the computing intensive part. Our gemm is implemented using a tiling strategy, this strategy improves data locality, thus enables the slow DDR transfer to keep up with the high throughput computing. In detail, the gemm is composed of three OpenCL kernels: MM, $Data_{in}$and $Data_{out}$. MM carries out the $tile \times tile$ task where the heavy computing lays. $Data_{in}$ kernel devides a the matrix A and B into tiles and sends them to MM. $Data_{out}$ receives the computing result as output tile from MM and write it back to DDR. Note that the matrix A, B, and C do not have to be stored in DDR as an actual matrix. $Data_{in}$ serves the role to virtualize matrices for MM, model specific logic and optimization are involved in this conversion process. $Data_{in}$ and $Data_{out}$ kernel obey certain protocol on DDR data layout, to make sure $Data_{out}$ output reused for next round's $Data_{in}$.

We first give a detailed description about our gemm structure and performance model, then we give two cases in our project on how gemm accelerates specific tasks.

5.2 GEMM details

There are two fectors affecting gemm performance: IO bandwidth and computing power. In case of our experiment, matrix is stored in DDR3 memory and computing power is 1024 DSP.

$$Bandwidth_{DDR} = 8GB/s$$

$$Bandwidth_{comp} = 1024DSP \times 200MHz = 204.8GB/s$$

This means IO can not keep up with computing in naive implementation. Our implementation solve this mismatch by exploring the data locality inside matrix multiplication. We fetch the matrix from DDR and buffer them on on chip block ram by tile. We configure block ram storage in a banked manner and feed data to computing units with high bandwidth. This strategy is shown in 5.

Figure 6 shows a general structure $Data_in$, MM, and $Data_out$. MM takes in tile of matrix A and tile of matrix B from $Data_in$, and performs tile multiplying tile. We generate resuce tree hardware to perform $V \times V$. In practice, multiple sets of $V \times V$ hardware could be generate and work simultaneously to increase throughput, this configuration is update to the user's trade off between resource usage and performance. Figure 6 shows the detailed structure inside MM. MM takes in two tiles of input matrices, and performs the tiled matrix multiplication in *Dot Product Unit* vector by vector. All the input data are fed into multipliers simultaneously, then the temporary results are summed up through a reduction tree to minimize the computing latency. In practice, N_{dot} *Dot Product Unit*s can be generated and work simultaneously to increase the overall throughput. This degree of parallelism is decided by the trade-off between resource utilization and performance. Denoting the multiplication length *Dot Product Unit* as L, we can estimate the performance (in OPS, operations per second) of MM in Equation **??**, where $Freq$ indicates the running frequency of FPGA board.

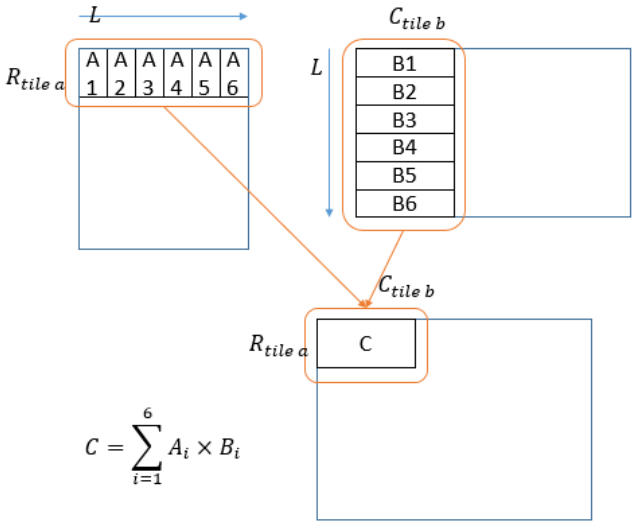

Figure 5: Tiling

Besides, we implement two set of buffers ($Buffer0$ and $Buffer1$ in Figure 6). Each buffer the tiled input data, and they operate in a ping-pong manner: During a certain phase, *Dot Product Unit* is processing with the tiles fetched from $Buffer0$, and the tiles to be processed in the next phase are loaded into $Buffer1$ simultaneously. Once *Dot Product Unit* finished computing with current tiles, it comes to the next phase, and every operation reverses. *Dot Product Unit* processes the tiles fetched from $Buffer1$, and $Buffer0$ loads the next tiles. In this manner, IO time consume could be hidden during computing.

In the tilig strategy, we use R_{tile_a} to denote row length of tile A, C_{tile_b} to denote column of tile B, L to denote column of tile A and row of tile B. L is also the vector dot product computing unit length. We use N_{dot} to denote number of dot product units we generate. We use $thrIO$ to denote IO throught, which is proportional to the DDR bandwidth, $thrComp$ to denote computing unit throughput, which is proportional to the computing power we invest to MM kernel (number of DSP). We have the following IO time consume and computing time consume comparasion:

$$thrComp = L \times N_{dot}$$

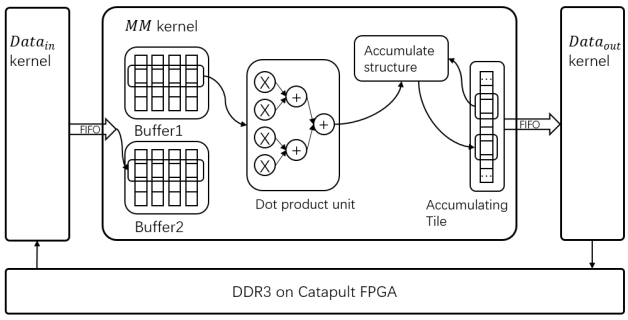

Figure 6: MM kernel

$$totalIO = R_{tile\_a} \times L + L \times C_{tile\_b}$$

$$totalComp = R_{tile\_a} \times C_{tile\_b} \times L$$

$$timeIO = totalIO/thrIO$$

$$timeComp = totalComp/thrComp$$

Note in the ping-pong manner, we require $timeIO < timeComp$ to keep the computation unstalled. This condition equals:

$$thrIO > thrComp \times (\frac{1}{R_{tile\_a}} + \frac{1}{C_{tile\_b}})$$

thrIO is FPGA board-specific and is always a constant. In our case it is 8GB/s, that is 64 8bit fix point numbers per cycle at 200MHz. This equision shows the following fact:

- Tile shape matters. For the certain bram resource ($R_{tile\_a} \times L$) to store a tile, the "narrower" tile shape we choose, the better data could be reused.
- The more computing unit we employ, the bigger tile size is needed. This could be intuitively explained as the tile multiplication is $O(N^2)$ IO V.S. $O(N^3)$ computing, the bigger tile size we choose, the more we take advantage of this property.

This exploration work can be accomplished by simple algorithms for integer programming problems. *Symbolic Compiler* in our framework can help to explore the design space and find the optimal hardware configuration.

5.3 MM Specialization

Deep learning models are constructed by many different types of layers, and the computation and data accessing pattern vary among these layers, so the strategies for converting them into MM are also quite different. We provide details about the converting methods in $Data_{in}$ and $Data_{out}$ for typical types of layers as follows.

5.4 GEMM Specialization Case 1: Convolution Layers

In cnn, most of the computing lays in convolution layers. N matrices called feature maps, and M filters are input to convolution layer. Each filter is consist of N subfilters, and each subfilter performs 2-D convolution through its correspondig input feature map. N convolution results are sum

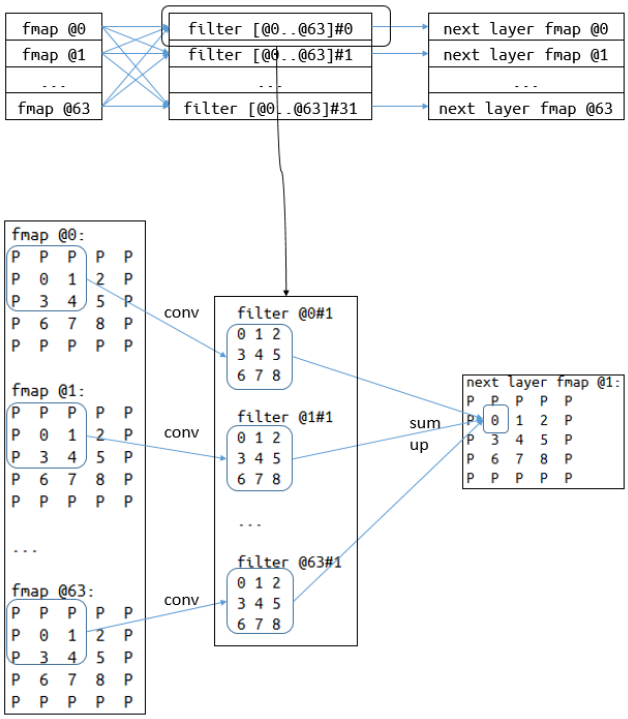

Figure 7: Convolution Layer

up to produce a output feature map. We use I to denote input feature map set, O for output feature map set. F to denote the filter set, the operation can be summarized as 1.

$$O_i = \sum_{j=1}^{M} conv(F_i^j, I_j) \quad (1)$$

Intuitively, for each output element's computing, we need the input elements it concerns to arrive at once. Only in this way can we stream the whole computing, otherwise massive on chip storage are needed of the intermediate results. Unfortunately, the total input elements that a single output element concerns are widely distributed, both inside a feature map and across feature maps. This could be shown in Figure 1, the computing of every output feature map involves two levels of DDR memory stride: 1) a single 2-D convolve operation strides across feature map rows. 2) Summing up convolve operation results strids across feature map. The two level stride leads non-trivial DDR performance problem: Fragmented DDR access wastes DDR burst transfer; Large strided DDR access making DDR frequently recharge. These factors make DDR transfer unable to keep up with computing even with the tiling strategy. On the other hand, we notice that considerable overlap exists between consecutive filter window sliding. We propose a DDR feature map layout, along with the its corresponding tiling strategy, that makes our gemm not only fetch from DDR sequencially, but also reuses the consecutive fetched tile.

Our strategy is shown in Figure 8, We use @ to denote input feature maps, # to denote filters (also output feature

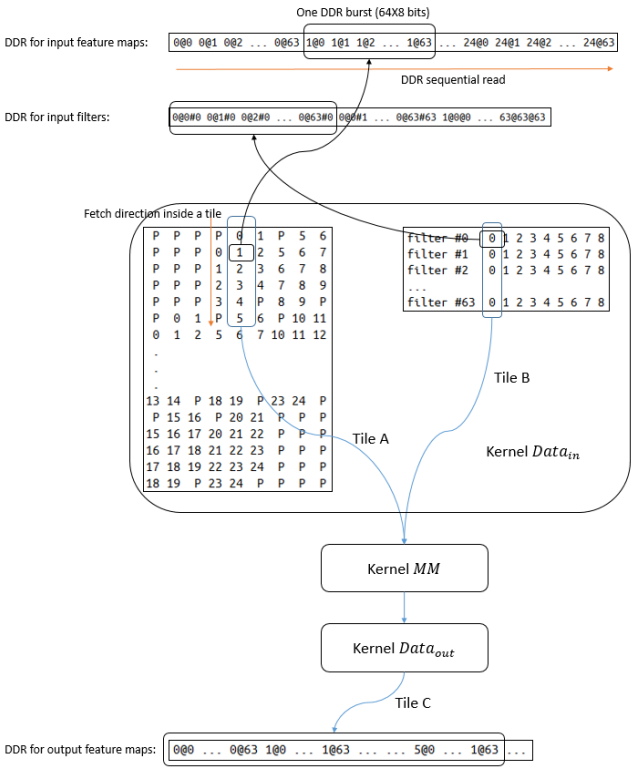

Figure 8: layout

maps). In our notation, 5@6 means the 5th element of the 6th input feature map; 6@7#4 means the 6th element of the 7th subfilter of the 4th filter; 7#4 means the 7th element of the 4th output feature map. P means padding in the target matrix (padded on the fly in kernel $Data_{in}$).

Suppose our tile A has size of R_{tilea} rows and L columns, we pack the elements at the same position of L feature maps together in DDR storage. Figure 8 shows that: Inside a row, L elements lays in sequential; Consecutive rows corresponds to consecutive feature map position, which are also sequential in DDR. When fetching a tile, we fetch row by row, so the entire fetching of a tile are sequential at DDR. Also, note that in Figure 8, most elements overlaps in three (the filter size in the general case) consecutive tiles, we just need to buffer the previous tile and fetch an extra element to cook up the next tile. This further saves nearly $(filter\_size - 1)/filter\_size$ DDR transfer.

5.5 GEMM Specialization Case 2: Recurrent Layers

In recent years, Long Short-Term Memory (LSTM) has gained great popularity in RNN design. These LSTM-RNNs use LSTM cells in their topological structure, and achieve state-of-art performance in several applications.

$$\begin{pmatrix} i \\ f \\ o \\ g \end{pmatrix} = \begin{pmatrix} sigmoid \\ sigmoid \\ sigmoid \\ tanh \end{pmatrix} W \times \begin{pmatrix} h_t^{l-1} \\ h_{t-1}^{l} \end{pmatrix} \tag{2}$$

$$c_t^l = f \odot c_{t-1}^l + i \odot g \tag{3}$$

$$h_t^l = o \odot tanh(c_t^l) \tag{4}$$

Equation 2 shows RNN mainly employs $M \times V$ (hidden state vector multiples weight matrix), this operation is inefficient in terms of data locality, for every weight element fetched from DDR is used only once. Recall that ..., we solve this problem by batching V in $M \times V$ as show in **??**, every element of W is reused $\#batch$ times.

$$M \times V \rightarrow M \times (V^1, V^2, \ldots, V^{\#batch})$$

As the mv problem is converted into mm problem, we could reuse our MM kernel.

Besides, several special stratety is took to implement the $Data_o ut$ kernel template for LSTM application, we take these strategy to explore the specific data flow property in LSTM model.

- Each gate vector element are used exactly once in element wise operation, (i_i, f_i, o_i, g_i) are used together to update vector c and h, this indicates that there is no need to buffer these vectors in $Data_o ut$. In practice, we arrange these vector as in Figure 9, MM kernel outputs (i_i, f_i, o_i, g_i) together and $Data_o ut$ consumes them immediately.
- The LSTM model adopts tanh and sigmoid as activation function, these functions are resource-expensive. We notice that activation takes small proportion of the whole computing operations, as could be shown in 2, it is $O(N)$ for activation and $O(N^2)$ for $M \times V$. Thus, small amount of activation computing units at kernel $Data_o ut$ will be enough to keep up with kernel MM. In our experiment, we have 1536 vector size V.S. 1024 multipler, one copy of activation function is enough. Taking advantage of this approach, we use fully precision version of sigmoid and tanh instead of interpolation version to promote the model accuracy. We insert a deep fifo with the capacity of an output tile between kernel MM and kernel $Data_o ut$, this fifo decomposes the computing process inside two kernels, making both kernels always work at full load asynchronously.

In this batching manner, we can easily convert matrix multiplying vector into matrix multiplication, and reuse MM to perform it. Besides, to further explore the specific data flow property of LSTM, we apply two special strategies to $Data_{out}$ for LSTM layers.

- Each gate vector element are used exactly once in element wise operation, (i_i, f_i, o_i, g_i) are used together to

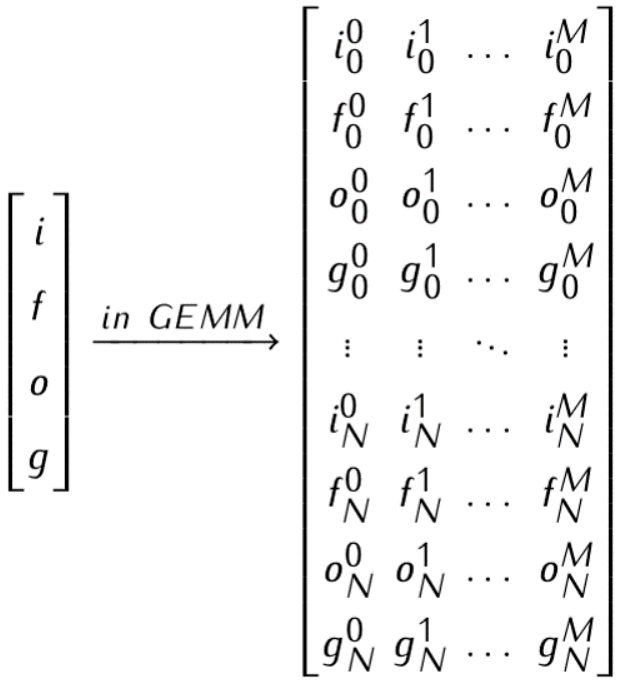

Figure 9: Crossed vector layout

update vector c and h, this indicates that there is no need to buffer these vectors in $Data_out$. In practice, we arrange these vector as in Figure 9, MM kernel outputs (i_i, f_i, o_i, g_i) together and $Data_out$ consumes them immediately.

- The LSTM model adopts tanh and sigmoid as activation function, these functions are resource-expensive. We notice that activation takes small proportion of the whole computing operations, as could be shown in 2, it is $O(N)$ for activation and $O(N^2)$ for $M \times V$. Thus, small amount of activation computing units at kernel $Data_out$ will be enough to keep up with kernel MM. In our experiment, we have 1536 vector size V.S. 1024 multipler, one copy of activation function is enough. Taking advantage of this approach, we use full-precision version of sigmoid and tanh instead of linear approximation in previous work [10] to promote the model accuracy. We insert a deep fifo with the capacity of an output tile between kernel MM and kernel $Data_out$, this fifo decomposes the computing process inside two kernels, making both kernels always work at full load asynchronously.

$Data_{out}$ will be enough to keep up with MM. Taking advantage of this approach, we use full-precision version of sigmoid and tanh instead of linear approximation in previous work [10]. We insert a deep FIFO with the capacity of an output tile between MM and $Data_{out}$, this FIFO decomposes the computing process inside two kernels, making both kernels always work at full load asynchronously.

5.6 Other Layers

5.6.1 Fully-Connected Layers

The inference phase of fully-connected layers can be summarized as Equation 5, (bias adding is omitted for simplicity). These layers output a vector (Out) as the multiplication of input vector (In) and weight matrix ($Weight$). Fully-connected layers are also widely deployed in deep learning models. Layers inside ANNs, classifiers inside modern CNNs, and recurrent layers inside simple RNNs are all in fact fully-connected layers. As a result, we apply the same implementation strategies to these layers and summarize in this section. As Equation 5, computation inside fully-connected layers can be viewed as matrix multiplying vector. Thus, we can use our MM kernel to perform it by similar strategies of LSTM layer.

$$Out[x] = \sum_{i=1}^{N_i} In[i] \ * \ Weight[x][i] \tag{5}$$

5.6.2 Activation Layers

The operations in activation layers are always element-wise operation, so there is no need to implement an extra kernel for it. We simply add them to $Data_{out}$ kernel before the outputs are written back to DDR. Note that the total number of activating operation is much less than $M \times M$ or $M \times V$ operation, so we put less resource to activation than GEMM without stalling the whole system's pipeline.

5.6.3 Pooling Layers

The operations performed in pooling layers can be summarized as Equation 6. Typically, pooling layers take the maximum (max-pooling) or the average (average-pooling) of the input features in a pooling window as the result to output. Pooling layers are always responsible for sub-sampling features. As shown in Equation 6, though not much computation is involved in pooling layers, pooling window usually strides on a 2D address space. As a result, it is quite complex to add pooling operations to $Data_{out}$ kernel, and we implement a individual pooling kernel instead for flexibility and extensibility.

$$Out[x][y] = \underset{0 \leqslant i,j < Size_{window}}{Pooling_{Max/Average}}(In[x+i][y+j]), \tag{6}$$

6. EVALUATION

Numerous prior works have shown that deep learning models are robust enough even with a decrease on data precision. Many great works [cite, cite,...] on accelerating deep learning model inference used fixed-point parameters in their design for performance improving and resource saving. Recently, Bengio et.al found that deep CNN models can even use binary values for model inference without much accuracy loss[cite]. So in our implementation, we also support implementing a fixed-point version of the target model. However, the accuracy loss brought by data quantization must be estimated and tested by the model designers in advance, and they need to make a decision on the trade-off between accuracy and performance.

To illustrate the effectiveness and great performance achieved by our proposed framework, we design and implement three models as our case studies for modern typical deep learning structures: ANN (or feedforward neural network), CNN, and RNN.

6.1 Experimental setup

For the software part, the *Symbolic Compiler* that performs performance estimation, resourse estimation, parameter decision, and OpenCL codes generation is written in Python X.X. To implement our desing on FPGA board, we take advantage of a high-level synthesis design tool, Altera AOCL (vXXX). This high-level synthesis tool help us synthesis and implement the OpenCL-based codes into binary files to program FPGA. The codes on host is written in C++, and compiled by Visual Studio XXX.

For the hardware part, we use a PikesPeak board, with an Altera Stratix-V GSMD5 FPGA on it. An 8GB DDR3 is integrated with the FPGA chip as external storage. The working frequency of hardware implementation is set to 200MHz. This FPGA board is plugged into a PCI-e slot of a host PC. The CPU inside host is XXXXX, XXGHz,

For performance comparison, we implement software inference on a Xeon CPU. It has XX cores and a XXMB L1 cache. The working frequency of it is xx GHz.

6.2 Experimental results

6.2.1 Performance

MM kernel is the core part of FPGA-based model inference, so we compared the performance of our MM kernel with other state-of-the-art implementations. We show the performance (in GOPS) of our implementations (floating-point and 8-bit fixed point), Intel MKL[] and Altera MM example design[] in Figure **??**. Our implementation and Altera MM example design run on the same FPGA board, and Intel MKL runs on the CPU introduced in Section 5.1. From Figure **??**, we can see that our 32-bit and 8-bit implementations of MM can outperform Intel MKL by XXx and XXx respectively, and the speed-ups on Altera MM example design is XXx and XXx on average.

To show the performance of our framework on a complete model, we compare our CNN implementations with previous accelerators, since there have been massive prior work on it. The comparison results are shown in Table 1. Note that numerous prior works have shown that deep learning models are robust enough even with a decrease on data precision. Many great works [17] [12] on accelerating deep learning model inference used fixed-point parameters in their design for performance improving and resource saving. Recently, Bengio et.al found that deep CNN models can even use binary values for model inference without much accuracy loss [13]. So in our implementation, we also support implementing a fixed-point version of the target model. Designers using our framework can enable it by simply adding a "$-fixed\_point$" compilation option to our *Symbolic Compiler*. However, the accuracy loss brought by data quantization must be estimated and tested by the model designers in advance, and they need to make a decision on the trade-off between accuracy and performance.

	ref	Our Imp	Our Imp
FPGA chip		Stratix-V GSMD5	
Frequency		200MHz	
CNN size		GOP	
Precision		float(32b)	fixed(8b)
Performance		GFLOPS	GOPS

Table 1: CNN performance comparison with prior work

Figure 10: energy efficiency comparison with cpu and gpu

6.2.2 Energy Efficiency

To show the great energy efficiency provided by our framework, we compare our implementations with those on CPU and GPU? in Figure 10. Several deep learning models are used as benchmarks: DSSM [cite] (ANN), VGG-19 [cite] (CNN), LSTM [cite] (RNN). The energy efficiency is measured in GOPS/W (giga ops per watt). Figure 10 shows that, in energy efficiency, our framework can outperform CPU by XXx and GPU by XXx on average.

6.2.3 Framework Effectiveness

For all the implemented models in Figure 10, our framework meanly takes about 4-5 hours to accomplish the hardware implementation from TensorFlow-described models. While it will take an experienced hardware engineer two weeks to implement one deep learning model on FPGA. So our framework can improve the efficiency of deep learning models' deployment by about 80x. Furthermore, designers with little knowledge about hardware implementation details can also easily use our framework, which indicates that our framework can be widely popularized and benefit the FPGA community.

The accuracy of the estimation models in *Symbolic Compiler* is evaluated in Figure 11. We show the comparison between estimated performance and measured performance of implemented models in Section 5.2.2, and we can see that our proposed models are accurate enough with only XX % error.

7. CONCLUSIONS AND FUTURE WORK

In this paper, we propose a framework that automatically migrates TensorFlow described deep learning models to FPGA implementation for inference acceleration. We also propose several performance models and resource estimations to choose the optimal design configuration. Our case studies show the great performance and effectiveness achieved by this framework.

Figure 11: comparison between estimation and measurement

However, there are still several directions for future research. First, we will go on working with a distributed version of this framework on an FPGA fabric. Second, we will adapt the kernels inside our framework to support emerging optimization techniques for deep learning models like pruning, binarization, etc. Last but not least, we will further extend our framework to model training.

8. REFERENCES

[1] M. Abadi, A. Agarwal, P. Barham, E. Brevdo, Z. Chen, C. Citro, G. S. Corrado, A. Davis, J. Dean, M. Devin, S. Ghemawat, I. Goodfellow, A. Harp, G. Irving, M. Isard, Y. Jia, R. Jozefowicz, L. Kaiser, M. Kudlur, J. Levenberg, D. Mané, R. Monga, S. Moore, D. Murray, C. Olah, M. Schuster, J. Shlens, B. Steiner, I. Sutskever, K. Talwar, P. Tucker, V. Vanhoucke, V. Vasudevan, F. Viégas, O. Vinyals, P. Warden, M. Wattenberg, M. Wicke, Y. Yu, and X. Zheng. TensorFlow: Large-scale machine learning on heterogeneous systems, 2015. Software available from tensorflow.org.

[2] F. Bastien, P. Lamblin, R. Pascanu, J. Bergstra, I. J. Goodfellow, A. Bergeron, N. Bouchard, and Y. Bengio. Theano: new features and speed improvements. Deep Learning and Unsupervised Feature Learning NIPS 2012 Workshop, 2012.

[3] Y. Chen, T. Luo, S. Liu, S. Zhang, L. He, J. Wang, L. Li, T. Chen, Z. Xu, N. Sun, et al. Dadiannao: A machine-learning supercomputer. In *Proceedings of the 47th Annual IEEE/ACM International Symposium on Microarchitecture*, pages 609–622. IEEE Computer Society, 2014.

[4] Y.-H. Chen, T. Krishna, J. Emer, and V. Sze. 14.5 eyeriss: An energy-efficient reconfigurable accelerator for deep convolutional neural networks. In *2016 IEEE International Solid-State Circuits Conference (ISSCC)*, pages 262–263. IEEE, 2016.

[5] A. Graves, A.-r. Mohamed, and G. Hinton. Speech recognition with deep recurrent neural networks. In *Acoustics, Speech and Signal Processing (ICASSP), 2013 IEEE International Conference on*, pages 6645–6649. IEEE, 2013.

[6] K. Greff, R. K. Srivastava, J. Koutník, B. R. Steunebrink, and J. Schmidhuber. Lstm: A search space odyssey. *arXiv preprint arXiv:1503.04069*, 2015.

[7] K. He, X. Zhang, S. Ren, and J. Sun. Deep residual learning for image recognition. *arXiv preprint arXiv:1512.03385*, 2015.

[8] Y. Jia, E. Shelhamer, J. Donahue, S. Karayev, J. Long, R. Girshick, S. Guadarrama, and T. Darrell. Caffe: Convolutional architecture for fast feature embedding. In *Proceedings of the ACM International Conference on Multimedia*, pages 675–678. ACM, 2014.

[9] H. Li, Z. Lin, X. Shen, J. Brandt, and G. Hua. A convolutional neural network cascade for face detection. In *Proceedings of the IEEE Conference on Computer Vision and Pattern Recognition*, pages 5325–5334, 2015.

[10] S. Li, C. Wu, H. Li, B. Li, Y. Wang, and Q. Qiu. Fpga acceleration of recurrent neural network based language model. In *Field-Programmable Custom Computing Machines (FCCM), 2015 IEEE 23rd Annual International Symposium on*, pages 111–118. IEEE, 2015.

[11] D. Liu, T. Chen, S. Liu, J. Zhou, S. Zhou, O. Teman, X. Feng, X. Zhou, and Y. Chen. Pudiannao: A polyvalent machine learning accelerator. In *Proceedings of the Twentieth International Conference on Architectural Support for Programming Languages and Operating Systems*, pages 369–381. ACM, 2015.

[12] J. Qiu, J. Wang, S. Yao, K. Guo, B. Li, E. Zhou, J. Yu, T. Tang, N. Xu, S. Song, et al. Going deeper with embedded fpga platform for convolutional neural network. In *Proceedings of the 2016 ACM/SIGDA International Symposium on Field-Programmable Gate Arrays*, pages 26–35. ACM, 2016.

[13] M. Rastegari, V. Ordonez, J. Redmon, and A. Farhadi. Xnor-net: Imagenet classification using binary convolutional neural networks. *arXiv preprint arXiv:1603.05279*, 2016.

[14] R. Sarikaya, G. E. Hinton, and A. Deoras. Application of deep belief networks for natural language understanding. *Audio, Speech, and Language Processing, IEEE/ACM Transactions on*, 22(4):778–784, 2014.

[15] J. Sim, J.-S. Park, M. Kim, D. Bae, Y. Choi, and L.-S. Kim. 14.6 a 1.42 tops/w deep convolutional neural network recognition processor for intelligent ioe systems. In *2016 IEEE International Solid-State Circuits Conference (ISSCC)*, pages 264–265. IEEE, 2016.

[16] K. Simonyan and A. Zisserman. Very deep convolutional networks for large-scale image recognition. *arXiv preprint arXiv:1409.1556*, 2014.

[17] N. Suda, V. Chandra, G. Dasika, A. Mohanty, Y. Ma, S. Vrudhula, J.-s. Seo, and Y. Cao. Throughput-optimized opencl-based fpga accelerator for large-scale convolutional neural networks. In *Proceedings of the 2016 ACM/SIGDA International Symposium on Field-Programmable Gate Arrays*, pages 16–25. ACM, 2016.

[18] W. Zaremba, I. Sutskever, and O. Vinyals. Recurrent neural network regularization. *arXiv preprint arXiv:1409.2329*, 2014.

[19] C. Zhang, P. Li, G. Sun, Y. Guan, B. Xiao, and J. Cong. Optimizing fpga-based accelerator design for deep convolutional neural networks. In *Proceedings of the 2015 ACM/SIGDA International Symposium on Field-Programmable Gate Arrays*, pages 161–170. ACM, 2015.